On the local structure of the glycyl radical in different enzymes

Fahmi Himo [a] **and Leif A. Eriksson** *[,a,b]

[a] *Department of Physics, Stockholm University, Box 6730, S-113 85 Stockholm, Sweden*
[b] *Department of Quantum Chemistry, Uppsala University, Box 518, S-751 20 Uppsala, Sweden*

2 PERKIN

Full hyperfine coupling tensors are computed for different geometric conformers of the glycyl radical, using gradient corrected Density Functional Theory (DFT) together with large basis sets (IGLO-III). Comparison is made with three enzymes in which the radical is present, namely *Escherichia coli* pyruvate formate lyase (PFL), *Escherichia coli* anaerobic ribonucleotide reductase (RNR) and bacteriophage T4 anaerobic RNR. The excellent agreement in hyperfine coupling constants between theory and experiment confirms again that the radical is a glycyl radical and that, although embedded in the protein, it maintains the planar gas phase structure in both *E. coli* PFL and *E. coli* RNR. In contrast to these two systems, we propose a non-planar structure for bacteriophage T4 anaerobic RNR, in order to explain the unusually high $A_{zz}(^{13}C_{\alpha})$ coupling (66 G) recently measured by Sjöberg *et al.*[18]

Introduction

Ever since the discovery of the tyrosyl radical in *Escherichia coli* ribonucleotide reductase (RNR),[1] protein radicals have received considerable interest. Tyrosyl radicals are now proven to exist in, *e.g.* RNR,[2] photosystem II (PSII),[3] galactose oxidase[4] and prostaglandin H synthase,[5] and tryptophan radicals have been detected in cytochrome c peroxidase (CcP),[6] mutant Y122F RNR[7] and DNA photolyase.[8] These two radicals share the common feature of having the spin almost entirely located on the ring system of the residues, *i.e.* far away from the protein backbone. In that sense the glycyl radical, the object of this study, is quite different. It is the first case where the radical is centered on the polypeptide backbone. It is now well established that glycyl radical is present in *E. coli* pyruvate formate-lyase (PFL),[9–12] *E. coli* anaerobic RNR[13–16] and bacteriophage T4 anaerobic RNR.[17,18] In PFL, the glycyl radical catalyses the entire reaction mechanism of cleaving pyruvate to form formate and acetyl-CoA later used in the Krebs cycle. As there is a lack of X-ray crystal data for the structures of these anaerobic proteins (only the peptide sequence is known), theoretical calculations are an important tool with which to understand the fundamental reaction mechanisms and interactions. Furthermore, since proteins are not static, an available crystal structure, although providing valuable information about the three dimensional structure of the system and possible sites of interaction, does not offer a full picture which can explain the modifications caused by changed oxidation states, substrate binding, reaction mechanisms, *etc.*

In PFL, Knappe and co-workers showed, using isotope labelling and site directed mutagenesis techniques, that the radical is centered on the C_{α}-atom of the Gly734 residue.[10] Using the same methods, Sjöberg and co-workers concluded that the anaerobic *E. coli* and bacteriophage T4 reductases contained a radical centered on the C_{α}-atom of the Gly681 and Gly580 residues, respectively.[16,18] Anaerobic *E. coli* RNR and PFL show some similarities. They both, for instance, cleave at the radical site upon exposure to O_2. Both have doublet-dominated EPR signals with a hyperfine splitting of 14–15 G, which is believed to originate from the H_{α} atom of the glycyl radical residue. The isotropic $^{13}C_{\alpha}$ hyperfine coupling (hfcc) is 15–21 G for both systems. Some distinguishing features do exist, however, such as the exchangeability of the H_{α} atom in PFL but not in anaerobic *E. coli* RNR, and the more complex substructure in the EPR spectrum of PFL. This is assumed to arise from two non-exchangeable protons in the adjacent residues (Ser733 and Tyr735). The isotropic hfcc of the Gly580 H_{α} proton in T4 RNR is similar to the other two systems. However, the A_{zz} coupling of $^{13}C_{\alpha}$ in T4 RNR is significantly larger than in *E. coli* RNR and PFL (66 G for T4 RNR compared to 46–50 and 49 G for the other two, respectively). The source of this deviation is addressed in some detail in the present study.

On the theoretical front, Yu and co-workers have in a recent study concluded that of all glycine derived from H-atom extraction (N-centered, O-centered and C-centered), the C-centered radicals are the energetically most favourable.[19] Barone and co-workers have in several papers[20–22] used their 'quantum mechanical protocol for open-shell systems' (post Hartree–Fock computations taking into account vibrational averaging effects) to study the glycine radical, $H_2NCHCOOH$. They concluded that only the planar or nearly planar conformations are energetically accessible due to effective π-electron delocalization. The very good agreement in isotropic hyperfine couplings between the experimental results from PFL and *E. coli* RNR indicates that the planarity of the structure in the proteins is not due to long-range effects.

In a series of papers, we have employed gradient corrected density functional theory (DFT)[23,24] to the study of electronic and hyperfine properties of biologically active radicals.[25–27] The particular form of DFT employed has proved to yield very accurate theoretical hyperfine properties of, especially, organic radicals.[25–31]

Computational details

All geometries, energies and hyperfine parameters are computed using gradient corrected density functional theory (DFT), as implemented in the linear combination of gaussian type orbitals—density functional theory (LCGTO-DFT) program deMon.[32] The gradient corrections are those by Perdew[33] for the correlation potential and by Perdew and Wang[34] for the exchange terms.

The calculations were performed in two steps. First, geometries were optimized using the double zeta plus valence polarization (DZVP) basis sets by Andzelm *et al.*,[35] followed by single point DFT-EPR calculations using the larger IGLO-III basis sets. These are based on Huzinagas 11s7p series,[36] very loosely contracted, and to which a double set of polarization functions are added.[37] For the fitting of the charge density and the approximate exchange-correlation potential, V_{xc}, we have

* E-mail: leifaxel@physto.se

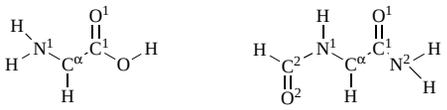

Glyrad Glyrad-ext

Fig. 1 Schematic representation of the two models of the glycine radical considered in the present study

used the auxiliary basis sets (5,1;5,1) for H and (5,2;5,2) for the remaining atoms.[38] The numbers given in parentheses describe the number of (s,spd) functions used for the charge density and V_{xc} fittings, respectively.

Results and discussion

Geometry

Two models of the glycine radical were employed (Fig. 1): the simple glycyl radical, $H_2NCHCOOH$ (hereafter called Glyrad) and a larger model extended to include parts of the backbone of neighbouring amino acids, CHO-NH-CH-CO-NH_2 (hereafter called Glyrad-ext). Geometry optimization gives, as expected, planar structures for both models, the only exception being two H atoms in the NH_2 moities, which are located slightly above the plane. The planarity of the molecules, which is due to effective electron delocalization, is in complete agreement with previous theoretical work.[19,20]

The effects of the geometry from extending the model are very minor (Table 1). The largest changes are the increase in the C_α–C_1 and C_1–O_1 bond lengths and the decrease in the C_α–N_1 bond. We notice that our approach generally generates slightly longer bond distances than both UHF[20] and UMP2.[19] This is a general feature of PWP86/DZVP geometries.

Spin distributions and hyperfine properties

In Table 2 we present the full hyperfine tensors as well as the total spin density distributions for the two models studied. Spin densities, obtained from Mülliken population analyses, are reported only for heavy atoms; the absolute spin densities are less than 0.04 for all hydrogen atoms. In both models a large amount of the unpaired spin density is located on the C_α-atom (0.58 and 0.66 for Glyrad and Glyrad-ext, respectively), which supports the experimental assignment of a C_α-centered radical. We also observe that the relatively high concentration of spin density on N_1 (0.24) in Glyrad decreases to 0.06 and redistributes on the outermost heavy atom when the model is extended to Glyrad-ext (0.06 on N_2, 0.08 on C_2 and 0.11 on O_2). Of course, the latter model should be the more appropriate one for glycyl radicals in proteins.

When going from Glyrad to Glyrad-ext the hyperfine structures are modified considerably. The isotropic component on $^{13}C_\alpha$, for instance, increases from 13.9 to 18.0 G while A_{iso} on H_α is lowered from −12.6 to −13.9 G, which both lead to a better overall agreement with the experimental values for the glycine radical in the three enzymes considered, Table 3. Also, the anisotropic couplings change by up to 4 G by the extension of the model. For the specific system of Bacteriophage T4 RNR, the experimentally reported A_{zz} component on C_α is very high (66 G), compared to both the two other proteins where it has been observed (49 and 46–50 G for *E. coli* PFL and RNR, respectively) and to our two models (48.2 and 54.8 G for Glyrad and Glyrad-ext, respectively). This discrepancy is discussed in detail in the next subsection.

As mentioned in the introduction, two non-exchangeable protons with hfcc of 4.5 and 6 G are observed in *E. coli* PFL. These were unassigned in the original work,[10] but the authors

Table 1 PWP86/DZVP optimized geometries (Å and °). Other theoretical results are included for comparison.

	Glyrad	Glyrad-ext	UHF/HD[a]	MP2/6-31 G(d)[b]
Distances				
C_α–C_1	1.441	1.461	1.445	1.434
C_1–O_1	1.248	1.255	1.234	1.233
C_1–O	1.387	—	—	1.364
C_1–N_2	—	1.392	1.357	—
O–H_O	0.983	—	—	—
C_α–N_1	1.380	1.372	1.379	1.358
C_α–H_α	1.089	1.090	1.066	—
N_1–C_2	—	1.392	1.362	—
C_2–O_2	—	1.234	1.215	—
Angles				
N_1–C_α–C_1	117.0	114.7	—	116.4
C_α–C_1–O_1	123.6	120.2	—	124.5
C_α–C_1–O	114.4	—	—	112.8
C_α–C_1–N_2	—	117.8	116.9	—
O_1–C_1–N_2	—	120.9	122.8	—
O_1–C_1–O	121.9	—	—	126.3
C_α–N_1–C_2	—	125.3	123.2	—
N_1–C_2–O_2	—	123.2	123.8	—
Dihedral angles				
N_1–C_α–C_1–O_1	4.8	−1.1	—	—
N_1–C_α–C_1–O	184.4	—	—	—
N_1–C_α–C_1–N_2	—	175.7	—	—
C_2–N_1–C_α–C_1	—	180.3	—	—
O_2–C_2–N_1–C_α	—	−1.0	0.0	—

[a] Ref. 20. HD = Dunning's [42/2] contraction of the Huzinaga (9s,5p/4s) basis. [b] Ref. 19.

Table 2 ^{13}C, ^{17}O, ^{14}N and ^{1}H hyperfine coupling tensors (G) for the two models investigated. Total spin densities on the heavy atoms, as calculated from Mulliken population analyses, are also included

	Glyrad					Glyrad-ext				
Atom	A_{iso}	T_{xx}	T_{yy}	T_{zz}	spin	A_{iso}	T_{xx}	T_{yy}	T_{zz}	spin
C_α	13.90	−17.26	−17.02	34.28	0.58	17.98	−18.65	−18.19	36.84	0.66
C_1	−6.71	−3.29	−1.82	5.11	0.06	−7.72	−1.37	−0.02	1.39	−0.01
O_1	−2.82	−15.00	7.47	7.53	0.14	−1.79	−11.34	5.59	5.75	0.11
O	−0.08	−5.57	2.47	3.10	0.04					
H_O	−1.38	−1.21	−1.01	2.22						
N_1	6.58	−4.49	−4.42	8.91	0.24	−0.90	−1.99	−1.82	3.81	0.06
$H_{N1\text{-}1}$	−1.72	−4.28	−1.89	6.17		−2.25	−1.59	−1.50	3.90	
$H_{N1\text{-}2}$	3.61	−5.34	−1.64	6.98						
H_α	−12.64	−8.27	−0.52	8.79		−13.88	−8.43	−0.41	8.83	
N_2						1.07	−1.09	−0.90	1.99	0.06
$H_{N2\text{-}1}$						−0.56	−1.21	−0.29	1.51	
$H_{N2\text{-}2}$						−0.71	−1.41	−0.63	2.04	
C_2						0.90	−2.42	−1.69	4.11	0.08
O_2						−2.45	−11.76	5.77	5.99	0.11
H_{C2}						−3.39	−1.67	−0.80	2.47	

Table 3 Selected hyperfine couplings (G) compared to their experimental counterparts. Note that experimentally, only absolute values are reported

hfcc	E. coli PFL[a] Gly-734	E. coli RNR[b] Gly-681	T4 RNR[c] Gly-580	Glyrad	Glyrad-ext
$A_{iso}(H_\alpha)$	15	14–15	14.4	−12.64	−13.88
$A_{xx}(^{13}C_\alpha)$	*ca.* 1	0.5	—	−3.36	−0.67
$A_{yy}(^{13}C_\alpha)$	*ca.* 2	0–5	—	−3.12	−0.21
$A_{zz}(^{13}C_\alpha)$	49	46–50	*ca.* 66	48.18	54.82
$A_{iso}(^{13}C_\alpha)$	16–21	15–21	—	13.90	17.98

[a] Ref. 10. [b] Ref. 16. [c] Ref. 18.

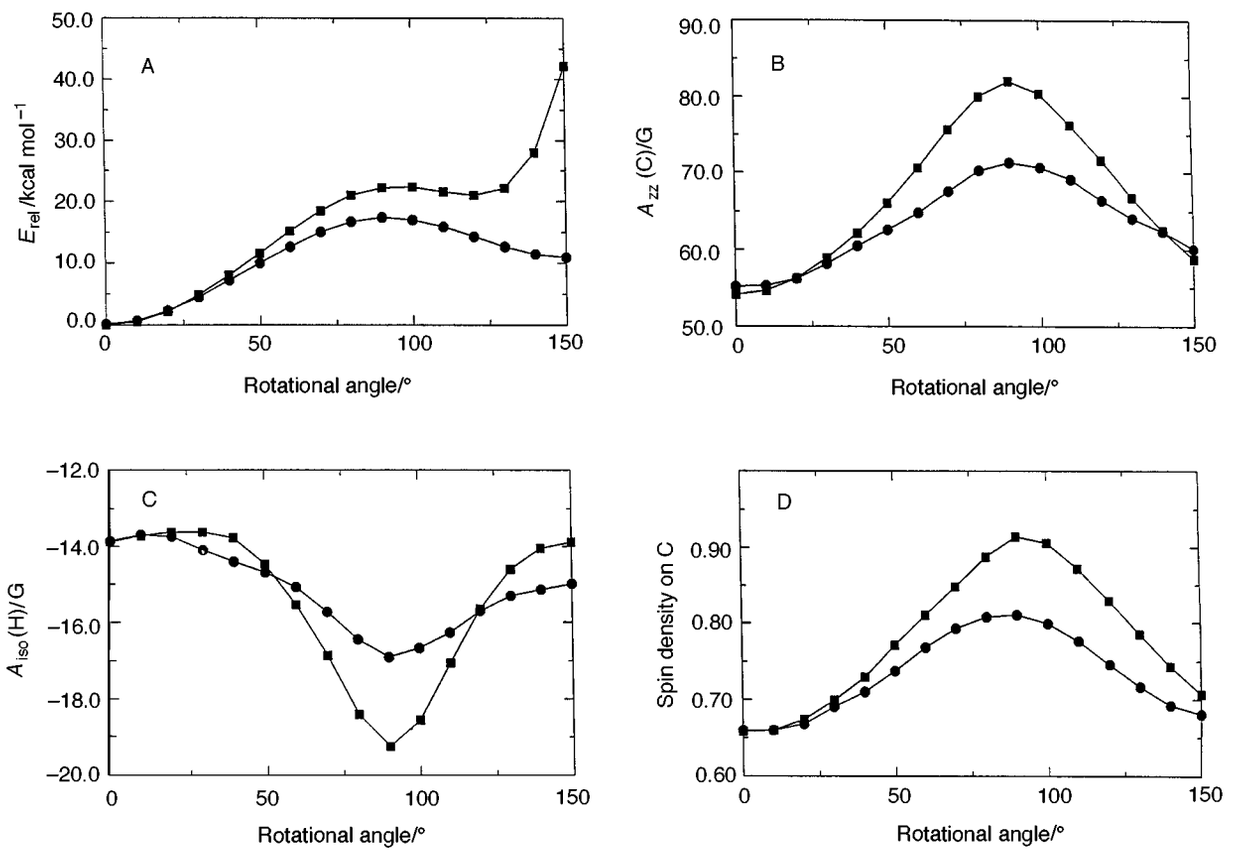

Fig. 2 Effects of rotations around C_α–C_1 (1) and around C_α–N_1 (2) on: (A) relative energy; (B) $A_{zz}(^{13}C_\alpha)$; (C) $A_{iso}(H_\alpha)$; (D) total spin density on C_α. (●) Rotation 1, (■) rotation 2.

speculated that the H_{N1}-proton or protons from adjacent residues could be the source of those couplings. From our calculation on Glyrad-ext, we note that the H_{N1}-proton, with $A_{xx} = 3.7$ G ($A_{iso} = -2.3$ G), could serve as a candidate for one of these protons. There is no proton coupling of a magnitude close to 6 G in this model, which supports the assumption that it originates from an adjacent residue. We are currently studying models of tripeptides (Ser-Glyrad-Tyr and Cys-Glyrad-Tyr), which we hope will lead to a more definite conclusion regarding the source of these two unassigned couplings.

Effects of rotations

The large discrepancy in $A_{zz}(C_\alpha)$ between theory and experiment for Bacteriophage T4 made us consider whether the geometry of the radical unit in this system is really planar. We therefore rotated the extended molecule around two different bonds, C_α–C_1 and C_α–N_1, in steps of 10° and at each point performed single point calculations at the PWP86/IGLO-III level of theory. The rotations were conducted up to 150° only, since further rotation will change the whole character of the molecule by creating bonds between the outermost atoms. The effects of the two rotations are displayed in Fig. 2.

The 66 G coupling of $A_{zz}(C_\alpha)$ is reproduced best for a rotational angle of *ca.* 60° for both rotations. The energy is then *ca.* 12–15 kcal mol^{-1} higher than the planar ground state structure. $A_{iso}(H_\alpha)$ is *ca.* −15 G, which is still in very good agreement with the experimental value (14.4 G) and the spin density on C_α increases to *ca.* 0.75. All changes in the other hfccs are within ±2 G for all dihedral angles covered. Relaxation of the structure during the rotation, *i.e.* optimizing all degrees of freedom except the dihedral angle considered, will lower the rotational energy by *ca.* 1–2 kcal mol^{-1}. The resulting 10 kcal mol^{-1} is still too high from the ground state structure, and the question of whether the three dimensional structure of the protein is able to 'force' the glycine radical to take an energetically unfavourable non-planar structure then arises. Our calculations indicate that this may indeed be the case. It is important to emphasize that we make no quantitative statement about the actual rotation of the radical, but rather a qualitative indication that the high 66 G coupling could have a structural explanation. The present model of rotation is naturally associated with some uncertainties, as we do not (for computational reasons) explicitly take structural reorganization into account. Such reorganization will in the present case involve lengthening of the rotated bonds due to breakage of conjugation; we do not, however, expect any considerable modifications of spin localization or spatial arrangement thereof at C_α. We should not, of course, exclude other explan-

ations of the observed deviating data set, such as the presence of hydrogen bonding groups or maybe simply erroneous experimental measurement and/or interpretation.

Conclusions

We have in the present study applied accurate DFT calculations to study the geometric and hyperfine properties of the glycyl radical. We obtain overall good agreement in hyperfine coupling constants with the three proteins in which the radical has been observed, namely *E. coli* pyruvate formate-lyase, *E. coli* anaerobic RNR and bacteriophage T4 anaerobic RNR. Based on a comparison of hfccs, we propose planar structures for the radicals in *E. coli* PFL and *E. coli* RNR, but most likely not in bacteriophage T4 anaerobic RNR.

Acknowledgements

We wish to thank Dr Britt-Marie Sjöberg and Dr Margareta Sahlin for most valuable discussions. The Swedish Natural Science Research Council (NFR) is also gratefully acknowledged for financial support.

References

1 P. Reichard and A. Ehrenberg, *Science*, 1983, **221**, 514.
2 C. W. Hoganson, M. Sahlin, B.-M. Sjöberg and G. T. Babcock, *J. Am. Chem. Soc.*, 1996, **118**, 4672.
3 B. E. Barry and G. T. Babcock, *Proc. Natl. Acad. Sci. USA*, 1987, **84**, 7099.
4 J. W. Whittaker, in *Metal Ions in Biological Systems*, *Volume 30: Metalloenzymes Involving Amino Acid-Residue and Related Radicals*, ed. H. Sigel and A. Sigel, Marcel Dekker, Inc., 1994, and references therein.
5 A. Tsai, R. J. Kulmacz and G. Palmer, *J. Biol. Chem.*, 1995, **270**, 10 503.
6 B. M. Hoffman, J. E. Roberts, C. H. Kang and E. Margoliash, *J. Biol. Chem.*, 1981, **256**, 6556.
7 M. Sahlin, G. Lassmann, S. Pötsch, A. Slaby, B. M. Sjöberg and A. Gräslund, *J. Biol. Chem.*, 1994, **269**, 11 699.
8 S. T. Kim, A. Sancar, C. Essenmacher and G. T. Babcock, *Proc. Natl. Acad. Sci. USA*, 1993, **90**, 8023.
9 J. Knappe, F. A. Neugebauer, H. P. Blaschkowski and M. Gänzler, *Proc. Natl. Acad. Sci. USA*, 1984, **81**, 1332.
10 A. F. V. Wagner, M. Frey, F. A. Neugebauer, W. Schäfer and J. Knappe, *Proc. Natl. Acad. Sci. USA*, 1992, **89**, 996.
11 M. Frey, M. Rothe, A. F. V. Wagner and J. Knappe, *J. Biol. Chem.*, 1994, **269**, 12 432.
12 C. V. Parast, K. K. Wong, S. A. Lewisch and J. W. Kozarich, *Biochemistry*, 1995, **34**, 2393.
13 X. Sun, J. Harder, M. Krook, B.-M. Sjöberg and P. Reichard, *Proc. Natl. Acad. Sci. USA*, 1993, **90**, 577.
14 E. Mulliez, M. Fontecave, J. Gaillard and P. Reichard, *J. Biol. Chem.*, 1993, **268**, 2296.
15 X. Sun, R. Eliasson, E. Pontis, J. Andersson, G. Buist, B.-M. Sjöberg and P. Reichard, *J. Biol. Chem.*, 1995, **270**, 2443.
16 X. Sun, S. Ollagnier, P. P. Schmidt, M. Atta, E. Mulliez, L. Lepape, R. Eliasson, A. Gräslund, M. Fontecave, P. Reichard and B.-M. Sjöberg, *J. Biol. Chem.*, 1996, **271**, 6827.
17 P. Young, M. Öhman and B.-M. Sjöberg, *J. Biol. Chem.*, 1994, **269**, 27 815.
18 P. Young, J. Andersson, M. Sahlin and B.-M. Sjöberg, *J. Biol. Chem.*, 1996, **271**, 20 770.
19 D. Yu and D. A. Armstrong, *J. Am. Chem. Soc.*, 1995, **117**, 1789.
20 V. Barone, C. Adamo, A. Grand, Y. Brunel and R. Subra, *J. Am. Chem. Soc.*, 1995, **117**, 1083.
21 V. Barone, C. Adamo, A. Grand and R. Subra, *Chem. Phys. Lett.*, 1995, **242**, 351.
22 V. Barone, C. Adamo, A. Grand, F. Jolibois, Y. Brunel and R. Subra, *J. Am. Chem. Soc.*, 1995, **117**, 12 618.
23 P. Hohenberg and W. Kohn, *Phys. Rev.*, 1964, **B136**, 864; W. Khon and L. J. Sham, *Phys. Rev.*, 1965, **A140**, 1133.
24 R. G. Parr and W. Yang, *Density Functional Theory of Atoms and Molecules*, Oxford University Press, New York, 1989.
25 F. Himo, A. Gräslund and L. A. Eriksson, *Biophys. J.*, 1997, **72**, 1556.
26 F. Himo and L. A. Eriksson, *J. Phys. Chem.*, in press.
27 L. A. Eriksson, F. Himo, P. E. M. Siegbahn and G. T. Babcock, *J. Phys. Chem.*, in press.
28 V. G. Malkin, O. L. Malkina, L. A. Eriksson and D. R. Salahub, *in Theoretical and Computational Chemistry*, *Vol. 2; Modern Density Functional Theory; A Tool for Chemistry*, ed. P. Politzer and J. M. Seminario, Elsevier, 1995, and references therein.
29 L. A. Eriksson, *Mol. Phys.*, 1997, **91**, 827; J. E. Gano, E. J. Jacob, P. Sekher, G. Subramaniam, L. A. Eriksson and D. Lenoir, *J. Org. Chem.*, 1996, **61**, 6739; N. Salhi-Benachenou, L. A. Eriksson and S. Lunell, *Acta. Chem. Scand.*, 1997, **51**, 636.
30 L. A. Eriksson, *in Density Functional Methods: Applications in Chemistry and Materials Science*, ed. M. Springborg, Wiley, 1997, and references therein.
31 L. A. Eriksson, V. G. Malkin, O. L. Malkina and D. R. Salahub, *J. Chem. Phys.*, 1993, **99**, 9756; L. A. Eriksson, O. L. Malkina, V. G. Malkin and D. R. Salahub, *J. Chem. Phys.*, 1994, **100**, 5066; L. A. Eriksson, V. G. Malkin, O. L. Malkina and D. R. Salahub, *Int. J. Quantum Chem.*, 1994, **52**, 879.
32 A. St-Amant and D. R. Salahub, *Chem. Phys. Lett.*, 1990, **169**, 387; A. St-Amant; Ph.D. Thesis, Université de Montréal, 1991; D. R. Salahub, R. Fournier, P. Mlynarski, I. Papai, A. St-Amant and J. Ushio, *in Density Functional Methods in Chemistry*, ed. J. Labanowski and J. Andzelm, Springer, New York, 1991; C. Daul, A. Goursot and D. R. Salahub, *in Grid Methods in Atomic and Molecular Quantum Calculations*, ed. C. Cerjan, Nato ASI C142, 1993.
33 J. P. Perdew, *Phys. Rev.*, 1986, **B33**, 8822; 1986, **B34**, 7406.
34 J. P. Perdew and Y. Wang, *Phys. Rev.*, 1986, **B33**, 8800.
35 N. Godbout, D. R. Salahub, J. Andzelm and E. Wimmer, *Can. J. Chem.*, 1992, **70**, 560.
36 S. J. Huzinaga, *Chem. Phys.*, 1965, **42**, 1293; S. Huzinaga and Y. Sakai, *J. Chem. Phys.*, 1969, **50**, 1371.
37 W. Kutzelnigg, U. Fleischer and M. Schindler, *in NMR—Basic Principles and Progress*, vol. 23, Springer-Verlag, Heidelberg, 1990.
38 F. Sim, D. R. Salahub, S. Chin and M. Dupuis, *J. Chem. Phys.*, 1991, **95**, 4317.

Paper 7/06138B
Received 21*st August* 1997
Accepted 31*st October* 1997